J. Appl. Environ. Biol. Sci., 6(4)164-176, 2016

ISSN: 2090-4274
Journal of Applied Environmental and Biological Sciences
www.textroad.com

Numerical Solution of MHD of Boundary Layer Flow of Nanofluid Fluids Due to Porous Stretching Surface

M. A. El-Hakiem

Presently: Department of Mathematics, College of Science, Al-Zulfi, Majmaah University, Saudi Arabia.
Department of Mathematics, College of Science, Aswan, Aswan University, Egypt.

Received: January 16, 2016
Accepted: April 11, 2016

ABSTRACT

In this study we have explored the numerical solution of MHD flow of an incompressible nanofluid towards a stretching surface. The obtained model of nonlinear partial differential equations is converted into a set of ordinary differential equations using an appropriate transformation. Shooting method is employed to solve the said system of boundary layer equations. Discussion of momentum, temperature and concentration profiles against emerging parameters like Prandtl number Pr, Brownian motion parameter Nb, thermophoresis parameter Nt, Lewis number Le, stretching parameter ε, Suction and injection parameter f_w. Tabulated values of local Nusselt number and sherwood number is an added feature with detailed discussion against different pertaining parameters. It is observed that Temperature profile $\theta(\eta)$ is higher for large values of Brownian motion parameter Nb thermophoresis parameter Nt and Suction and injection parameter f_w. It is also found that for increasing values of magnetic field parameter M and velocity ratio parameter ε, skin friction coefficient show increasing and decreasing behavior respectively.

KEYWORDS: MHD; incompressible nano fluid; boundary layer; shooting method; stretching sheet.

1. INTRODUCTION

In many engineering and industrial processes, enhanced energy transfer rate has been a long time problem for the manufacturing of a refined product. "Nanofluids" are being preferred to the ordinary base fluid due their better thermal performance. "Nanofluid" are suspended fluids with suspended nanoparticles, with enhanced thermal conductivity and better cooling rate. Kuznetsov and Nield [1] examined natural convective boundary-layer flow of a nanofluid past a vertical plate. Khlebtsov et al. [2] studied the effect of the size, shape and structure of metal nanoparticles on the dependence of their optical properties on the refractive index of a disperse medium. Oztopa and Abu-Nada [3] studied numerically the natural convection in partially heated rectangular enclosures filled with nanofluids. Shehzad et al. [4] investigated MHD flow of Jeffrey nanofluid with convective boundary conditions. Hayat et al. [5] analyzed MHD three-dimensional flow of Maxwell fluid with variable thermal conductivity and heat source/sink. Abbasbandy et al [6] obtained numerical and analytical solutions for Falkner-Skan flow of MHD Oldroyd-B fluid. Ellahi and Hameed [7] presented Numerical analysis of steady non-Newtonian flows with heat transfer analysis, MHD and nonlinear slip effects. Turgut, et al. [8] thermal conductivity and viscosity measurements of water-based TiO2 nanofluid. Rudyak et al. [9] investigated the thermal conductivity of nanofluids. Murugesan and Sivan [10] discussed the limits of thermal conductivity of nanofluids. Ahmad and Pop [11] considered mixed convection boundary layer flow from a vertical flat plate embedded in a porous medium filled with nanofluids. Neild and Kuznetsov [12] studied the Cheng-Minkowycz problem for natural convective boundary-layer flow in a porous medium saturated by a nanofluid. Kuznetsov and Neild [13] examined natural convective boundary-layer flow of a nanofluid past, a vertical plate.

In controlling the quality of the refined product, the importance of heat transfer cannot be denied which highly depend on stretching and cooling rates. Khan and Pop [14] investigated the boundary layer flow of nanofluid past a stretching sheet. Bachok et al. [15] considered boundary layer flow of nanofluid over moving surface in a flowing fluid. Rana and R. Bhargava [16] examined the flow and heat transfer of a nanofluid over a nonlinearly stretching sheet. Arfin et al. [17] studied the viscous flow due to a permeable stretching/shrinking sheet in a nanofluid. Rahman et al [18] discussed the boundary layer flow of a nanofluid past a permeable exponentially shrinking surface with convective boundary condition using Buongiorno's model. Afify et al. [19] used scaling group transformation for MHD boundary layer flow over permeable stretching sheet in presence of slip flow with Newtonian heating effects. Ramzan and Bilal [20] considered time dependent MHD nano-second grade fluid flow induced by permeable vertical sheet with mixed convection and thermal radiation.

Corresponding Author: M. A. El-Hakiem, Presently: Department of Mathematics, College of Science, Al-Zulfi, Majmaah University, Saudi Arabia. Department of Mathematics, College of Science, Aswan, Aswan University, Egypt.

In this article, we obtained numerical solution of MHD flow of an incompressible nanofluid towards a stretching surface. The results have been obtained by using an easy and straight forward numerical schem. The effects of the physical parameters involved in the study have been observed on velocity, microrotation and concentration.

2. Mathematical Formulation

We consider a time independent two dimensional an incompressible nano viscous fluid flow over a stretching sheet. The external and stretching velocities $u_e(x) = ax$ and $u_w(x) = bx$ are considered respectively with a and b as positive constants. Effects of Newtonian heating are also considered here. Temperature and concentration at the surface are T_w and C_w whereas ambient temperature and concentration are T_∞ and C_∞ respectively. The governing boundary layer equations representing the system are:

$$\frac{\partial u}{\partial x} + \frac{\partial v}{\partial y} = 0 \tag{1}$$

$$u\frac{\partial u}{\partial x} + v\frac{\partial u}{\partial y} = \nu\frac{\partial^2 u}{\partial y^2} - \frac{\sigma B_0^2 u}{\rho} \tag{2}$$

$$u\frac{\partial T}{\partial x} + v\frac{\partial T}{\partial y} = \alpha\frac{\partial^2 T}{\partial y^2} + \left[D_B\frac{\partial C}{\partial y}\frac{\partial T}{\partial y} + \frac{D_T}{T_\infty}\left(\frac{\partial T}{\partial y}\right)^2\right] \tag{3}$$

$$u\frac{\partial C}{\partial x} + v\frac{\partial C}{\partial y} = D_B\frac{\partial^2 T}{\partial y^2} + \frac{D_T}{T_\infty}\frac{\partial^2 T}{\partial y^2} \tag{4}$$

with the boundary conditions

$$u = \pm u_w(x) \quad v = v_w,\ T = T_w,\ \ C = C_w \ \text{ at } \ y = 0$$
$$u = u_e(x) \quad T = T_\infty,\ \ C = C_\infty \ \text{ at } \ y \to \infty \tag{5}$$

Here u and v denote the velocity components in the x and y directions respectively, T and C are the temperature and concentration. D_B, D_T, and α are the Brownian diffusion coefficient, the thermophoretic diffusion coefficient, and the thermal diffusivity respectively. In order to find a similarity solution of equations [1-5], we use the following transformations:

$$\eta = \sqrt{\left(\frac{a}{\nu}\right)}\,y,\quad \Psi = \sqrt{a\nu}\,x f(\eta),\ \theta(\eta) = \frac{T - T_\infty}{T_\infty},\ (\eta) = \frac{C - C_\infty}{C_\infty}, \tag{6}$$

with the velocity components

$$u = \frac{\partial \Psi}{\partial y},\quad v = -\frac{\partial \Psi}{\partial x} \tag{7}$$

Equation (1) is identically satisfied while equations (2) to (5) are given by

$$f''' + ff'' - (f')^2 - Mf' = 0 \tag{8}$$

$$\theta'' + \Pr[f\theta' + Nb\theta'\phi' + Nt(\theta')^2] = 0 \tag{9}$$

$$\phi'' + Lef\phi' + \frac{Nt}{Nb}\theta'' = 0 \tag{10}$$

$$f(0) = \pm f_w,\quad f'(0) = \varepsilon,\ \theta(0) = 1,\ \ \phi(0) = 1,\ \eta = 0$$
$$f'(\infty) = 1,\ \theta(\infty) = 0,\ \ \phi(\infty) = 0,\ \eta \to \infty \tag{11}$$

where prime denotes differentiation with respect to η and $Pr, Le, Nb, Nt, M\ and\ \varepsilon$ denoted Prandtl number, Lewis number, Brownain motion parameter, Thermophoresis parameter, Magnetic field parameter and ratio parameter, respectively. These parameters are defined as:

$$Pr = \frac{\nu}{\alpha},\ Le = \frac{\nu}{D_B},\ Nb = \frac{D_B C_\infty}{\nu},\ Nt = \frac{D_T}{\nu},\ M = \frac{\sigma B_0^2}{\rho a},\ \varepsilon = \frac{b}{a} \tag{12}$$

The physical quantities as skin friction coefficient, Nusselt and Sherwood numbers are given by:

$$c_{fx} = -\frac{\sqrt{\nu}}{a^{3/2}x}\frac{\partial u}{\partial y}\bigg|_{y=0} = -f''(0),\ N_{ux} = \frac{x}{T_w - T_\infty}\frac{\partial T}{\partial y}\bigg|_{y=0} = -\frac{\theta\prime(0)}{\theta(0)},\ Sh_x = \frac{x}{C_w - C_\infty}\frac{\partial C}{\partial y}\bigg|_{y=0} = -\frac{\phi\prime(0)}{\phi(0)} \tag{13}$$

3 RESULTS AND DISCUSSION

The numerical solution of equations (8 − 10) with (11) has been found via shooting method to observe the effects of the parameters namely, Nb, Nt, ε, Pr, and Le. A comparison of the values of surface temperature $\theta(0)$, and heat transfer coefficient $-\theta'(0)$ has been made to authenticate results obtained from the method used. Table I

depicts the values of skin friction $f''(0)$, heat transfer coefficient $-\theta'(0)$, and mas transfer coefficient $-\phi'(0)$ under the various values of *M, Pr. Le,* f*w, ε, Nt,* and *Nb.* The results for velocity, temperature and concentration functions have been presented in graphical form.

Fig.1 demonstrates the inverted parabolic shape of velocity curves that decrease in magnitude with increase in the value of magnetic parameter M. It is because the Lorentz force decelerates the fluid flow. Fig.2 and fig.3 depict a slight increase in the values of $\theta(\eta)$ and $\phi(\eta)$ with increase in the values of M. The prandtl number Pr decreases the temperature distribution as shown in fig.4 but it increases concentration function slightly as depicted in fig.5. The Brownian motion parameter B_r has increasing effect on $\theta(\eta)$ but it has decreasing effect on $\phi(\eta)$as shown in fig.6 and fig.7 respectively. Fig.8 and fig.9 respectively show that the thermophoresis parameter N_t has slightly decreasing effect on $\theta(\eta)$ but significant increasing effect on $\phi(\eta)$. Fig.10 and fig.11 respectively demonstrate that Lewis number Le increases $\theta(\eta)$ but it decreases $\phi(\eta)$. Fig.12 show that the velocity ratio parameter ε increases the fluid velocity $f'(\eta)$ but it decreases $\theta(\eta)$ and $\phi(\eta)$ as shown in fig.13 and fig.14 respectively. Fig.15 depicts that the suction parameter f_w decreases the fluid velocity near the surface and it increases the velocity away from the surface but reciprocal effect is observed in fig.16 for injection. Fig.17 and fig.18 respectively demonstrate that $\theta(\eta)$ and $\phi(\eta)$decrease with increase in suction but Fig.19 and Fig. 20 respectively depict that $\theta(\eta)$ and $\phi(\eta)$ increases with increase in injection.

Table I

M	***Pr***	***Le***	**fw**	ε	***Nt***	***Nb***	$-f''(0)$	$-\theta'(0)$	$-\phi'(0)$
0.0	5.0	1.0	0.0	1.0	0.01	0.1	0.66510	1.42761	0.69542
0.2							0.77703	1.40980	0.68779
0.4							0.88298	1.39255	0.68067
0.5							0.93385	1.38413	0.67729
0.7							1.03163	1.36770	0.67089
0.9							1.12447	1.35182	0.66492
	7						0.77703	1.62828	0.66768
	10							1.88373	0.64402
	20							2.42968	0.59289
	50							3.10841	0.52873
	100							3.33389	0.50821
		2.0					0.77703	1.35307	0.95993
		5.0						1.25259	1.60112
		10						1.17987	2.34617
		20						1.12111	3.39975
			0.2				0.81368	2.03449	0.74726
			0.4				0.85037	2.73602	0.80747
			0.6				0.88689	3.49281	0.87019
			0.8				0.92306	4.28877	0.93645
			1.0				0.95871	5.11252	1.00668
			-0.2				0.74064	0.88773	0.62661
			-0.4				0.70473	0.49206	0.56133
			-0.6				0.66951	0.23207	0.49110
			-0.8				0.63522	0.09074	0.41806
			-1.0				0.60202	0.02926	0.34680
				2.0			2.64142	1.95844	0.81363
				3.0			5.02250	2.39288	0.92988
				4.0			7.83131	2.76172	1.03704
				5.0			11.01258	3.08735	1.13633
					0.02		0.77703	1.39255	0.60439
					0.04			1.35849	0.44720
					0.06			1.32504	0.30254
					0.08			1.29217	0.17008
						0.2	0.77703	1.20264	0.74095
						0.4		0.84521	0.76610
						0.6		0.56528	0.77321
						0.8		0.35898	0.77588

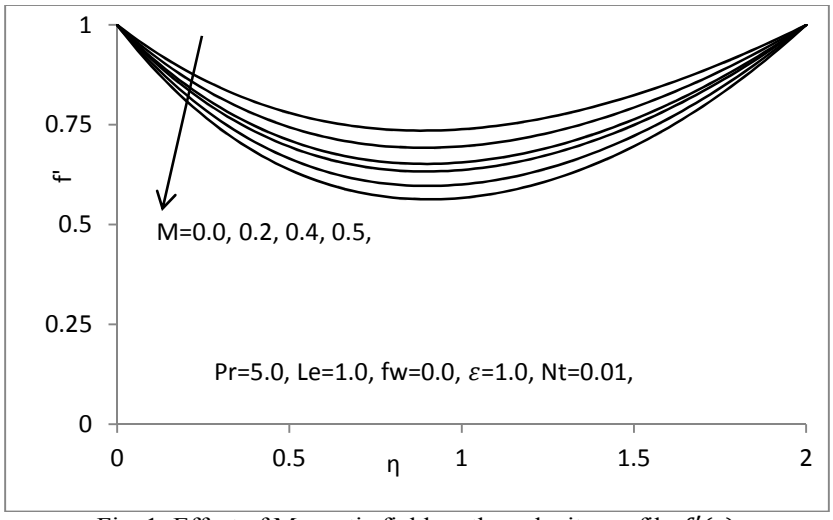

Fig. 1: Effect of Magnetic field on the velocity profile $f'(\eta)$

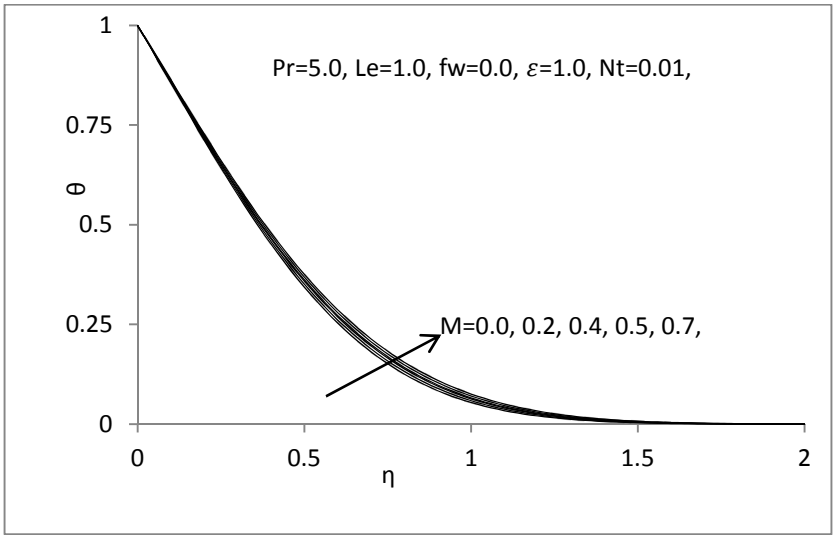

Fig. 2: Effect of Magnetic field on the temperature profile $\theta(\eta)$

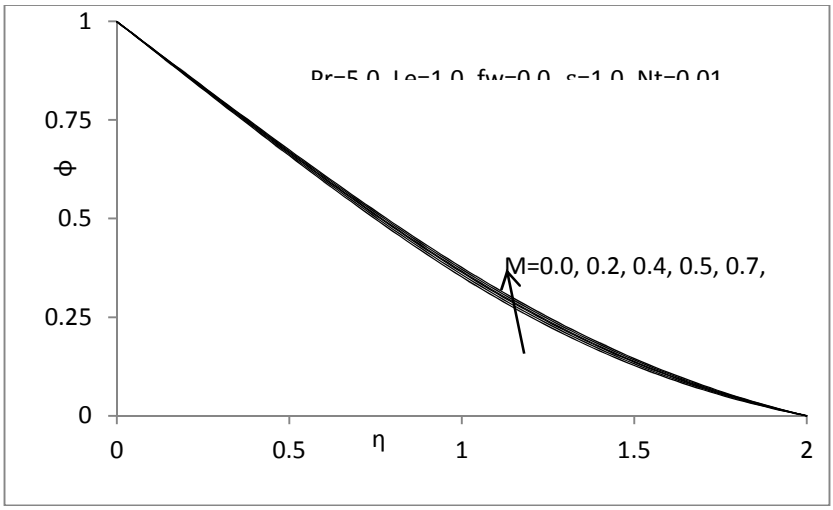

Fig. 3: Effect of Magnetic field on the concentration profiles $\phi(\eta)$

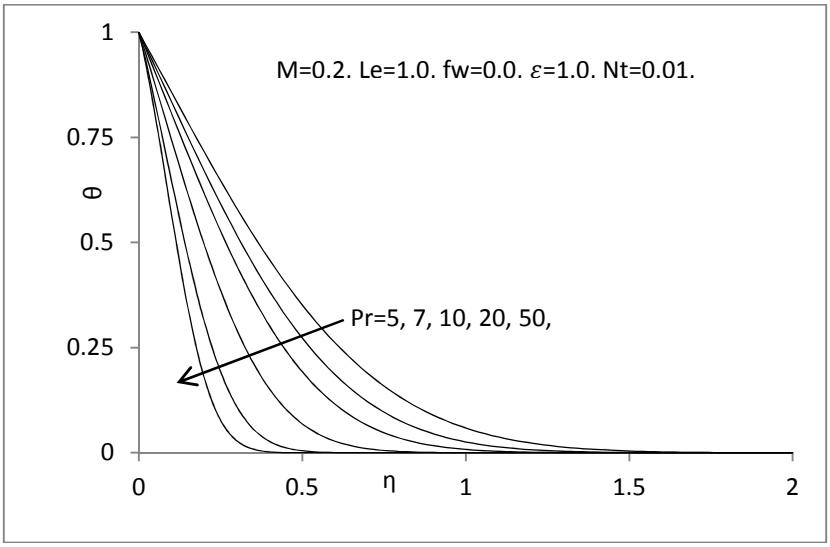

Fig. 4: Effect of Prandtl number *Pr* on the temperature profile $\theta(\eta)$

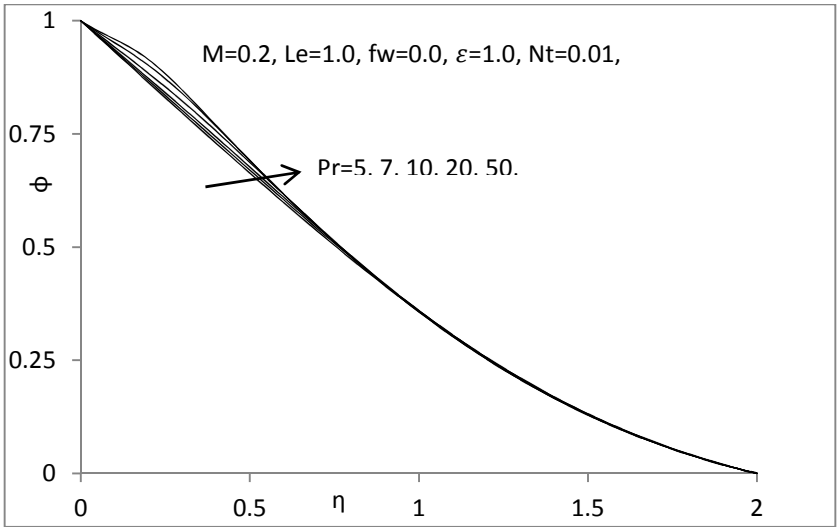

Fig. 5: Effect of Prandtl number *Pr* on the concentration profile $\phi(\eta)$

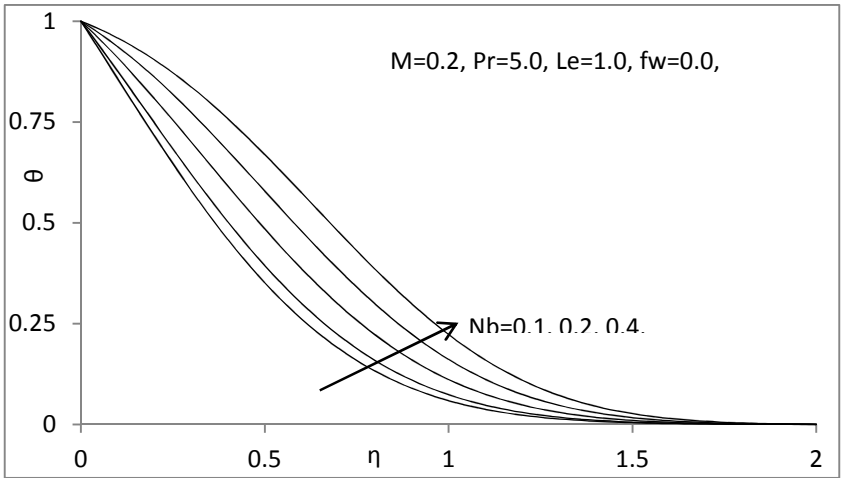

Fig. 6: Effect of Brownian motion parameter *Nb* on the temperature profile $\theta(\eta)$

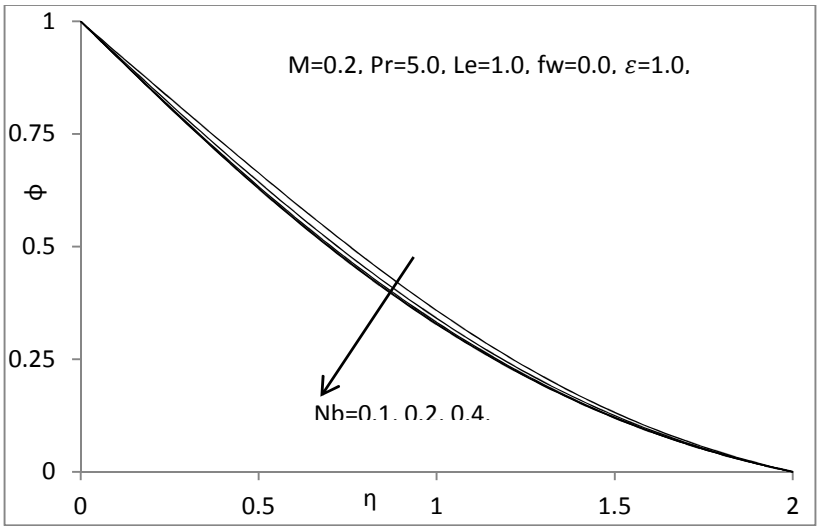

Fig. 7: Effect of Brownian motion parameter *Nb* on the concentration profile $\phi(\eta)$

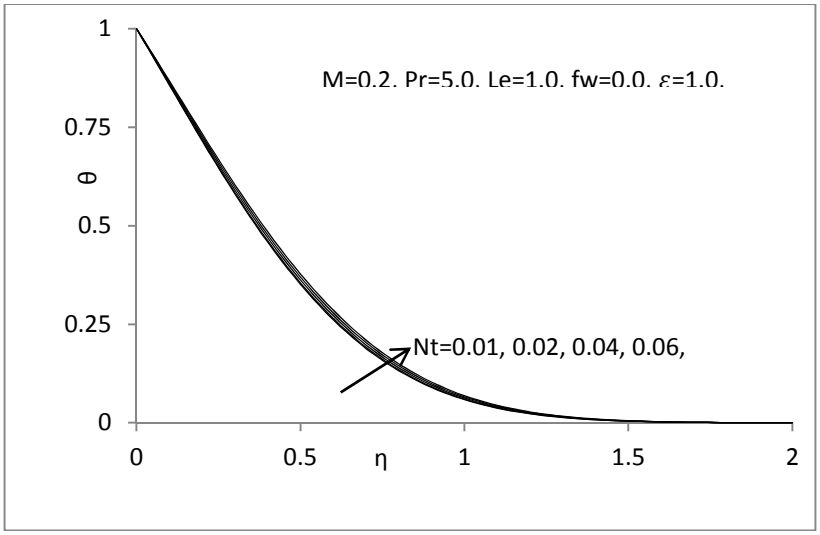

Fig. 8: Effect of thermophoresis parameter *Nt* on the temperature profile $\theta(\eta)$

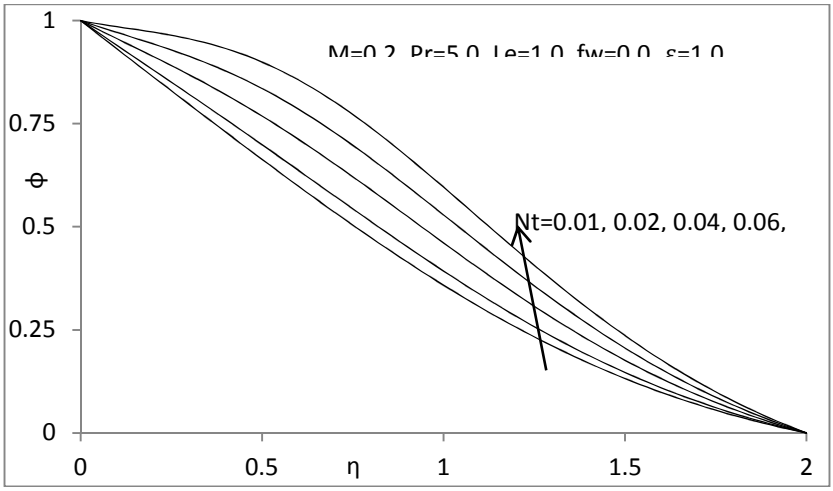

Fig. 9: Effect of thermophoresis parameter *Nt* on the the concentration profile $\phi(\eta)$

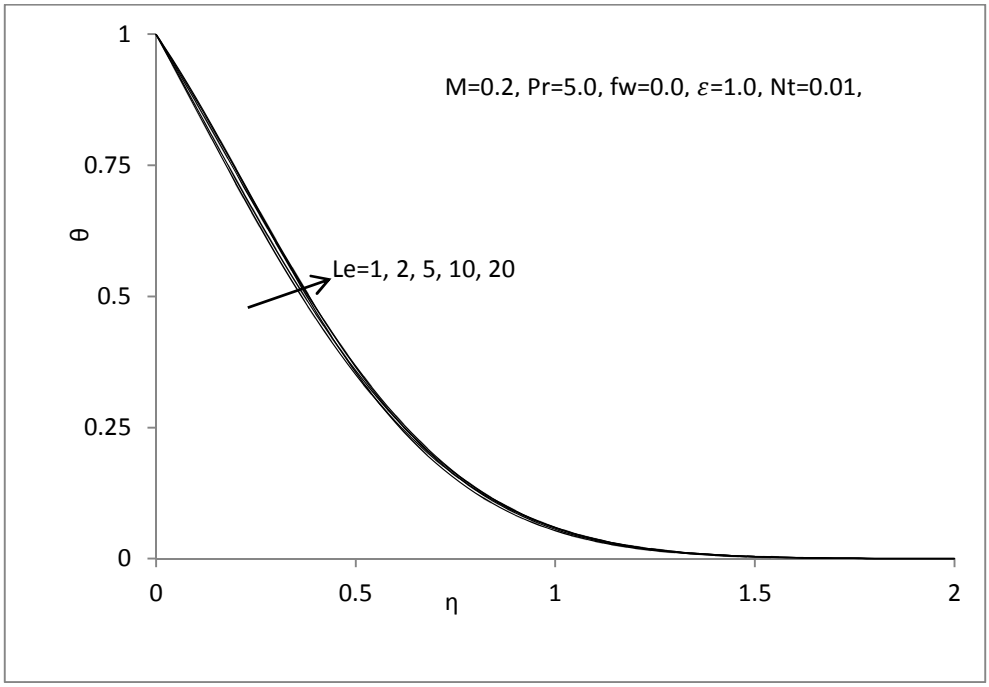

Fig. 10: Effect of Lewis number *Le* on the temperature profile $\theta(\eta)$

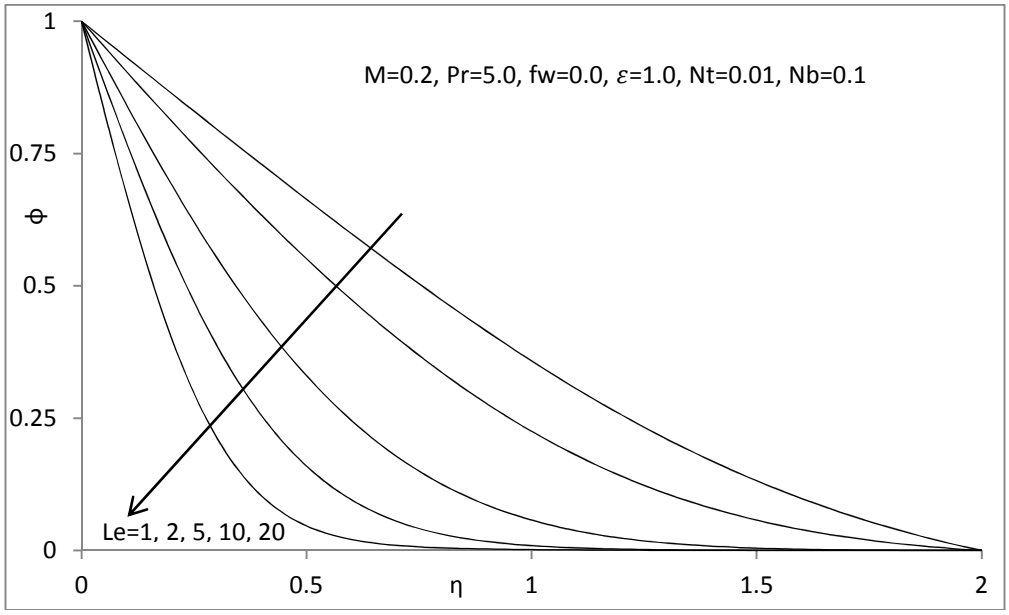

Fig. 11: Effect of Lewis number *Le* on the concentration profile $\phi(\eta)$

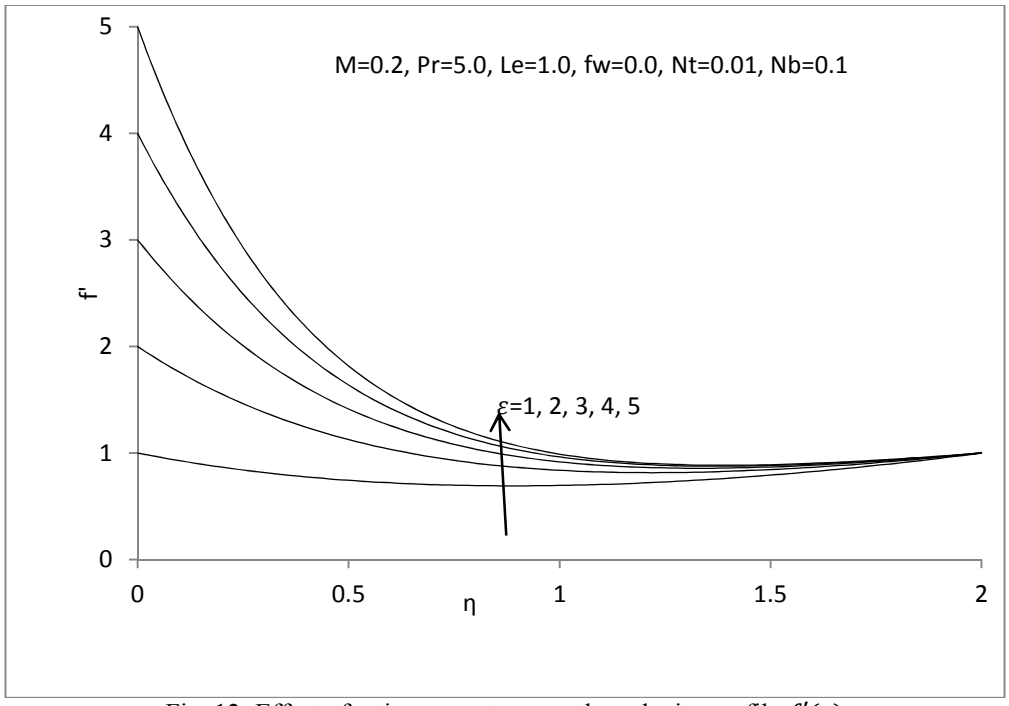

Fig. 12: Effect of ratio parameter ε on the velocity profile $f'(\eta)$

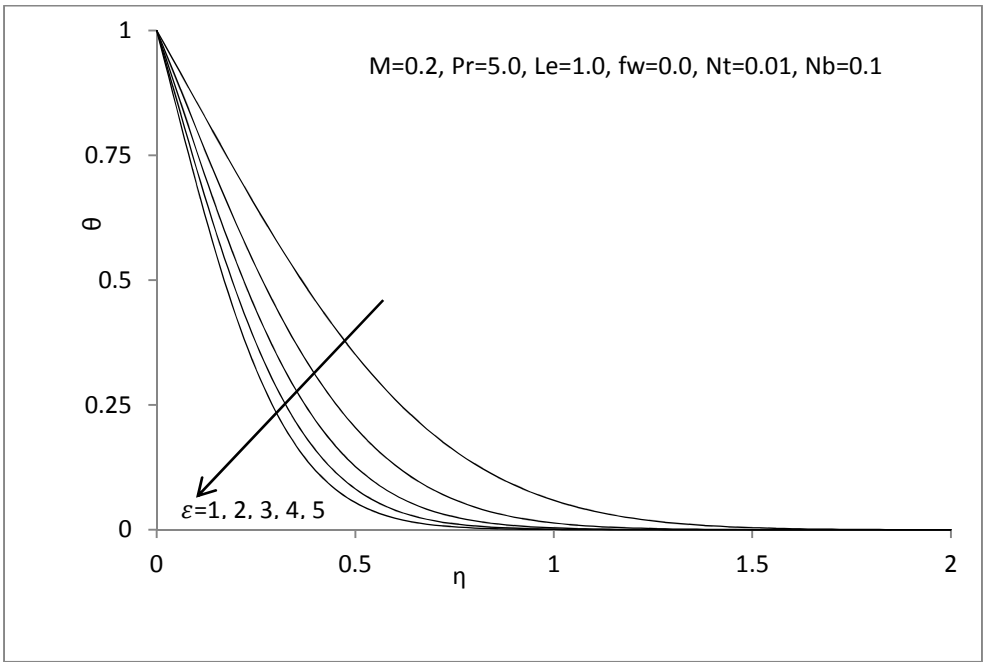

Fig. 13: Effect of ratio parameter ε on the temperature profile $\theta(\eta)$

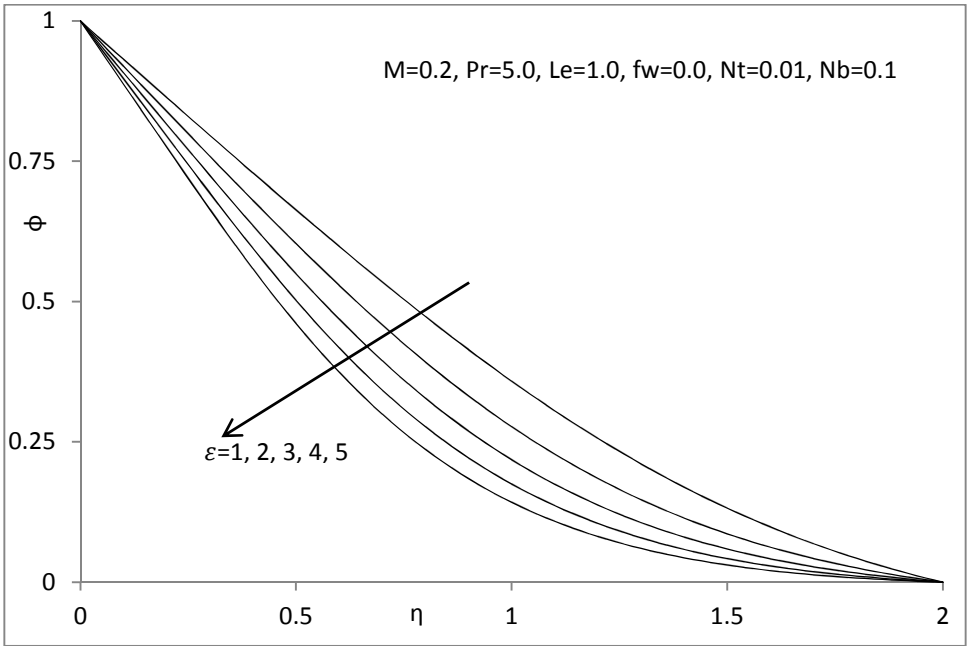

Fig. 14: Effect of ratio parameter ε on the concentration profile $\phi(\eta)$

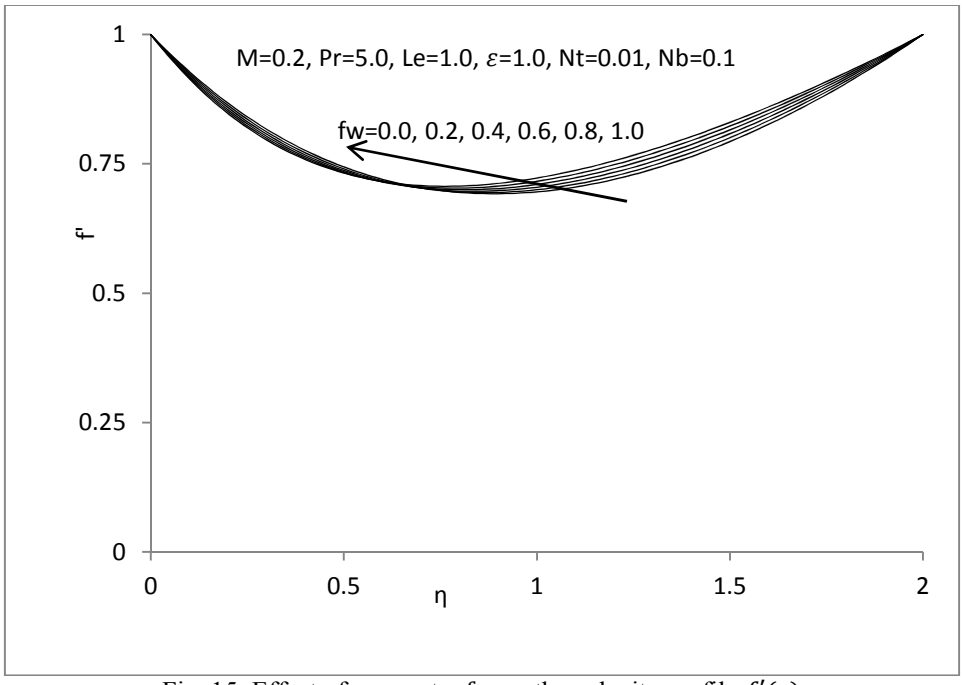

Fig. 15: Effect of parameter fw on the velocity profile $f'(\eta)$

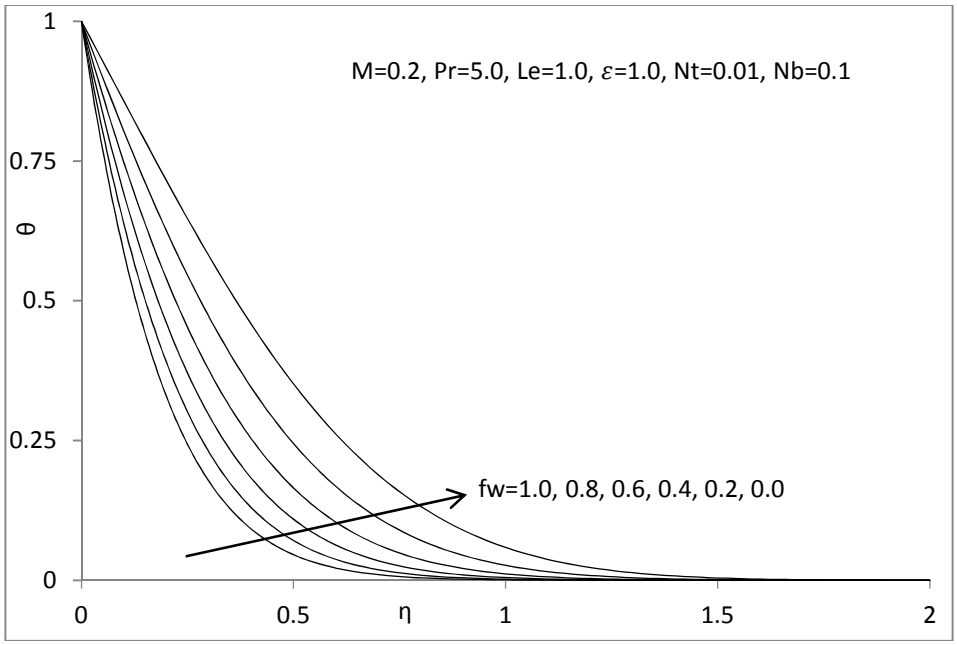

Fig. 16: Effect of the parameter f*w* on the temperature profile $\theta(\eta)$

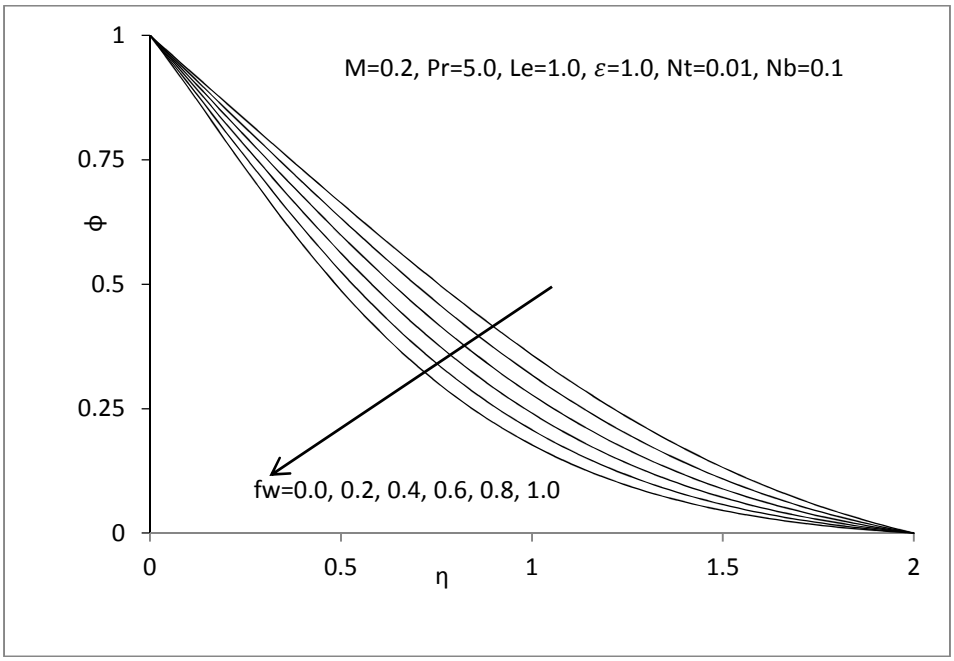

Fig. 17: Effect of the parameter fw on the concentration profile $\phi(\eta)$

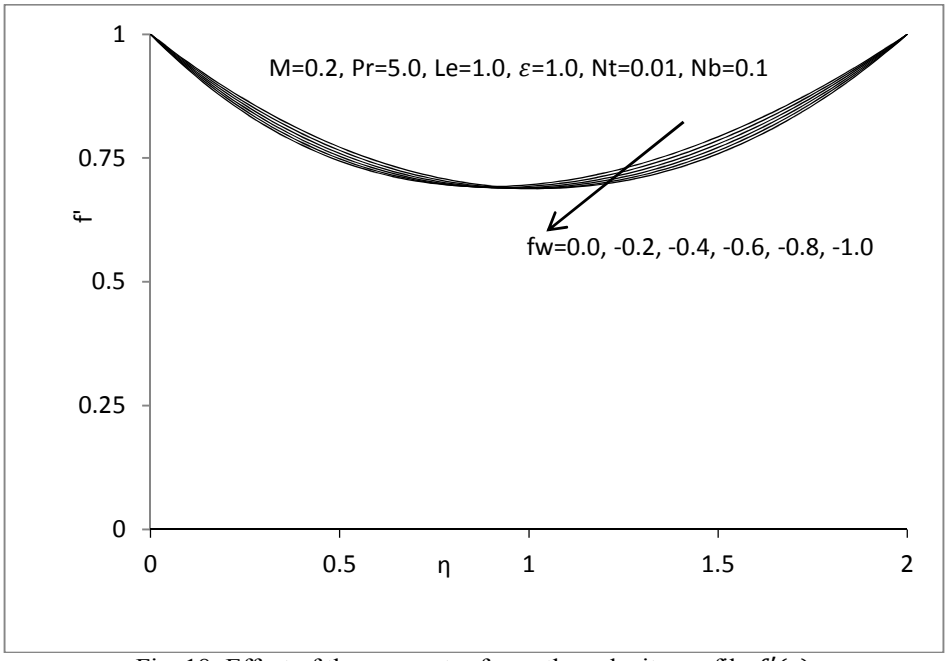

Fig. 18: Effect of the parameter f*w* on the velocity profile $f'(\eta)$

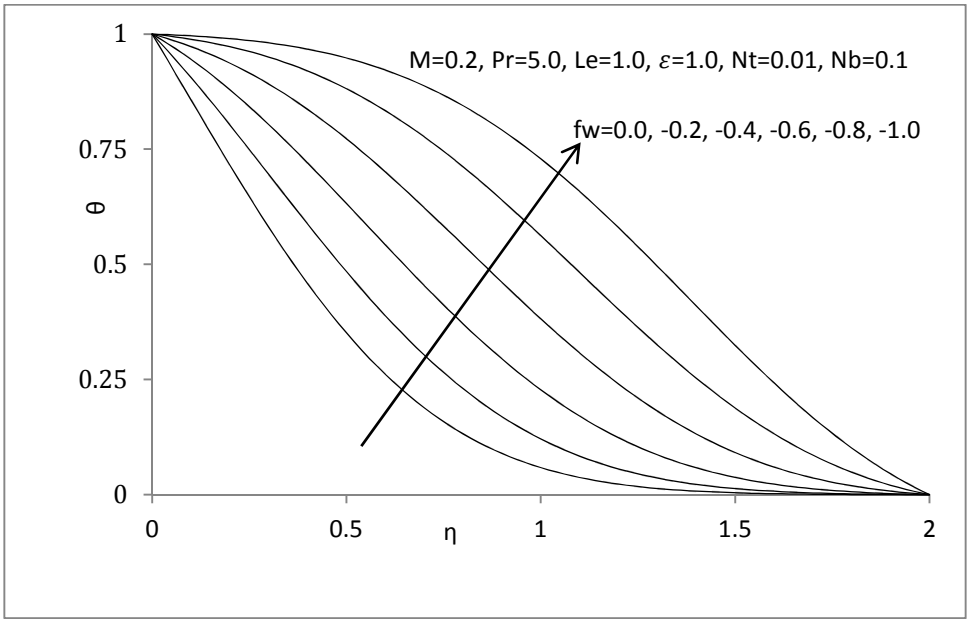

Fig. 19: Effect of the parameter f*w* on the temperature profile $\theta(\eta)$

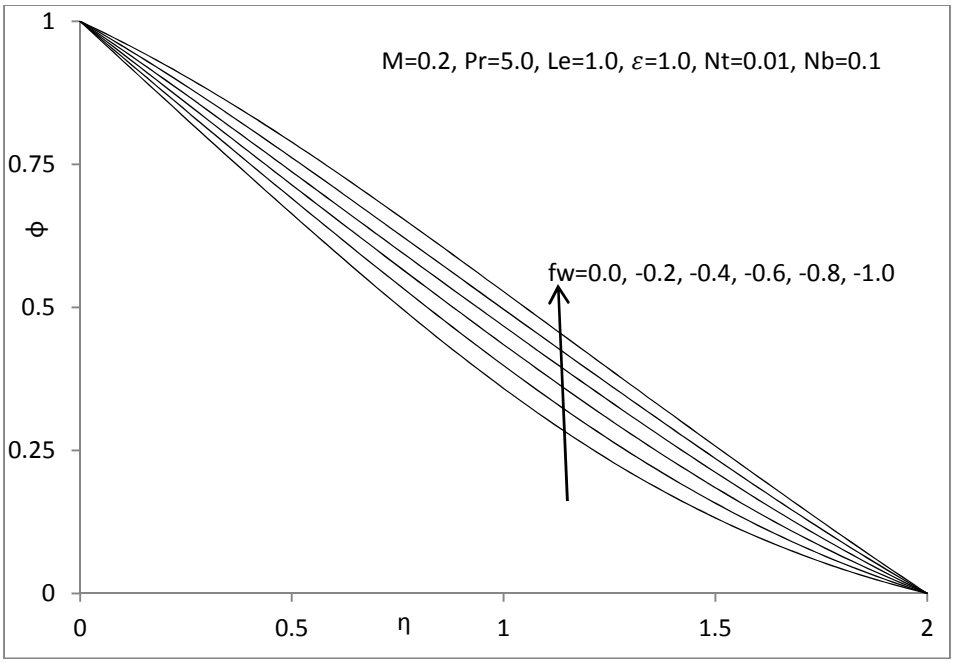

Fig. 20: Effect of the parameter fw on the concentration profile $\phi(\eta)$

4. **Conclusion**

The numerical solution of MHD flow of an incompressible nanofluid towards a stretching surface has been investigated to observe the effects of the physical parameters of the study on fluid flow and heat transfer phenomena. The main results of this work are summarized below:

- The velocity $f'(\eta)$ decreases in magnitude with increase in the value of magnetic parameter M.
- The values of $\theta(\eta)$ and $\phi(\eta)$ increase slightly with increase in the values of M.
- The prandtl number Pr decreases the temperature distribution but it increases concentration function slightly
- The Brownian motion parameter B_r has increasing effect on $\theta(\eta)$ but it has decreasing effect on $\phi(\eta)$.
- The thermophoresis parameter N_t has slightly decreasing effect on $\theta(\eta)$ but significant increasing effect on $\phi(\eta)$.
- Lewis number Le increases $\theta(\eta)$ but it decreases $\phi(\eta)$.
- The velocity ratio parameter ε increases the fluid velocity $f'(\eta)$ but it decreases $\theta(\eta)$ and $\phi(\eta)$.
- The suction parameter f_w decreases the fluid velocity near the surface and it increases the velocity away from the surface but reciprocal effect is observed for injection.

The functions $\theta(\eta)$ and $\phi(\eta)$decrease with increase in suction but these quantities increases with increase in injection.

Acknowledgment: This project was supported by the deanship of scientific research at Majmaah University under the research project No. 9. The author are highly grateful to Majmaah University, Deanship of Scientific Research and Research Center for Engineering and Applied Sciences, Majmaah University for support and encouragement.
The author is also, obliged to College of Science in Al-Zulfi City, Majmaah University, KSA) for sparing to accomplish this work. The author would like to thank Deanship of Scientific Research, Majmaah University, Kingdom of Saudi Arabia for funding this work under project number No.1436-2-9. (9. 1436).

REFERENCES

[1] A. V. Kuznetsov, D. A. Nield. (2010), Natural convective boundary-layer flow of a nanofluid past a vertical plate, International Journal of Thermal Science s vol. 49, pp. 243-247.
[2] N. G. Khlebtsov, L. A. Trachuk, A. G. Melnikov. (2005), the effect of the size, shape and structure of metal nanoparticles on the dependence of their optical properties on the refractive index of a disperse medium, Optics and Spectroscopy, vol. 98, pp. 77-83.

[3] H. F. Oztopa, E. Abu-Nada. (2008), Numerical study of natural convection in partially heated rectangular enclosures filled with nanofluids", International Journal of Heat and Fluid Flow, Vol. 29, No. 5, pp. 1326—1336.

[4] S. A. Shehzad, T. Hayat and A. Alsaedi. (2015), "MHD flow of Jeffrey nanofluid with convective boundary conditions", Journal of the Brazilian Society of Mechanical Sciences and Engineering, Vol. 37, No. 3, pp. 873 - 883.

[5] T. Hayat, S. A. Shehzad and A. Alsaedi. (2014), "MHD three-dimensional flow of Maxwell fluid with variable thermal conductivity and heat source/sink", International Journal of Numerical Methods for Heat & Fluid Flow, Vol. 24, No. 5, pp. 1073 - 1085.

[6] S. Abbasbandy, T. Hayat, T, Alsaedi, and M. M. Rashidi. (2014), Numerical and analytical solutions for Falkner-Skan flow of MHD Oldroyd-B fluid", International Journal of Numerical Methods for Heat & Fluid Flow, Vol. 24, No. 2, pp. 390 - 401.

[7] Ellahi, R; Hameed, M. (2012), "Numerical analysis of steady non-Newtonian flows with heat transfer analysis, MHD and nonlinear slip effects", International Journal of Numerical Methods for Heat & Fluid Flow, Vol. 22, No. 1, pp. 24 - 38.

[8] A. Turgut, et al. (2009), Thermal conductivity and viscosity measurements of water-based TiO2 nanofluid, International Thermophysics, vol. 30(40), pp. 1213-1226.

[9] V. Y. Rudyak, A. A. Belkin and E. A. Tomilina. (2010), on the thermal conductivity of nanofluids Technical Physics Letter, 36(7) 660-662.

[10] C. Murugesan and S. Sivan. (2010), Limits of thermal conductivity of nanofluids, Thermal Science, 14(1), 65-71.

[11] S. Ahmad and I. Pop. (2010), Mixed convection boundary layer flow from a vertical flat plate embedded in a porous medium filled with nanofluids, International Communications in Heat and Mass Transfer, 37, 987-991.

[12] D. A. Neild and A. V. Kuznetsov. (2009), The Cheng-Minkowycz problem for natural convective boundary-layer flow in a porous medium saturated by a nanofluid, International Communications in Heat and Mass Transfer, 52, 5692-5695.

[13] A. V. Kuznetsov and D. A. Neild. (2010), Natural convective boundary-layer flow of a nanofluid past, a vertical plate, International Journal of Thermal Science, 49, 243-247.

[14] W. A. Khan, I. Pop, Boundary layer flow of nanofluid past a stretching sheet. (2010), Int. J. of Heat and Mass Transfer, vol. 53, pp. 2477-2483.

[15] N. Bachok, A. Ishak, I. Pop. (2010), Boundary layer flow of nanofluid over moving surface in a flowing fluid, Int. J. Thermal Science s, vol. 49, pp. 1663-1668.

[16] P. Rana and R. Bhargava. (2012), Flow and heat transfer of a nanofluid over a nonlinearly stretching sheet, A numerical study of Communication in Nonlinear Science and Numerical Simulation, 17, 212-226.

[17] N. Arfin, R. Nazar and I. Pop. (2011), Viscous flow due to a permeable stretching/shrinking sheet in a nanofluid, Sains Malaysiana, 40(12), 1359-1366.

[18] M. M. Rahman, A. V. Rosca, I. Pop. (2015), "Boundary layer flow of a nanofluid past a permeable exponentially shrinking surface with convective boundary condition using Buongiorno's model", International Journal of Numerical Methods for Heat & Fluid Flow, Vol. 25, No. 2, pp. 299.

[19] A. A. Afify, M J. Uddin, M. Ferdows. (2014), "Scaling group transformation for MHD boundary layer flow over permeable stretching sheet in presence of slip flow with Newtonian heating effects", Applied Mathematics and Mechanics, Vol. 35, No. 11, pp. 1375 - 1386.

[20] M. Ramzan and M. Bilal. (2015), "Time dependent MHD nano-second grade fluid flow induced by permeable vertical sheet with mixed convection and thermal radiation", PLoS 1, Vol. 10, No. 5, pp. e0124929.